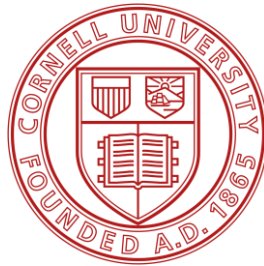


Treating Osteoporosis: Localized Drug Delivery into Femur

Gustavo Anaya, Jennifer Jackson, Zachary Roga, Andy Wu

Keywords: BP, bone, diffusion, alendronate, scaffold

BEE 4530: Computer-Aided Engineering: Applications to Biological Processes



Department of Biological and Environmental Engineering

Cornell University

© May 11, 2017

Table of Contents

Executive Summary	3
Introduction	3
Background	3
Problem Statement	4
Design Objectives	4
Problem Schematic	5
Methods	7
Governing Equations	8
Boundary and Initial Conditions	8
Implementation and Mesh Design	9
Results and Analysis	9
Mesh Convergence	9
Model Validation	11
Optimization	12
Sensitivity Analysis	12
Conclusions	14
Appendix A	15
Parameters	15
Appendix B	16
CPU Time	16
References	17

Executive Summary

Key words: BP, bone, diffusion, alendronate, scaffold

Bisphosphonates (BPs) are used to mitigate osteoporosis in patients who are at high risk for bone fractures. Common methods of administration of BPs rely on systemic delivery, which can lead to abdominal discomfort and unwanted concentrations of drug in other areas of the body. However, there is a limited understanding of the diffusion of BPs via localized delivery from scaffolds. This study investigates the diffusion of alendronate, a commonly used BP, from a scaffold into bone.

A model for diffusion with fluid flow was constructed using the commercially available computational software COMSOL. The femur bone is approximated as a 3D cylinder of length 0.1 m with four layered subdomains: scaffold, periosteum, compact bone, and marrow. The layers are of radius 0.0002 meters, 0.00022 meters, 0.001 meters, and 0.0138 meters respectively. BPs have a diffusion constant of $115 \cdot 10^{-12}$ square meters per second, $2.44 \cdot 10^{-10}$ square meters per second, $2.44 \cdot 10^{-10}$ square meters per second, and $1 \cdot 10^{-12}$ square meters per second respectively in the four layers of the domain. The periosteum and compact bone have capillaries that run the length of the domain. These are modeled as randomly distributed identical cylinders running the length of the domain with a unidirectional fluid flow of $5 \cdot 10^{-5}$ meters per second with a fluid density of 1060 kilograms per cubic meter. The initial conditions are concentration of 0 everywhere except for the scaffold subdomain which has an initial

concentration of 0.018 moles of alendronate per cubic meter of bone. These values can be found in Appendix A, Table 2.

The results of this model show the concentration of bound alendronate in the bone reaches an effective concentration of $1 \cdot 10^{-4}$ moles per cubic meter before 10 hours. We have also found the bound alendronate fraction has a low dependency on the initial scaffold concentration with the bound alendronate fraction at over 90% alendronate clearance time being over 0.8 for varying initial concentrations.

Sensitivity analysis revealed that bound alendronate concentration is not dependent on the diffusivities of compact bone or marrow, or on blood velocity, but is highly dependent on initial scaffold concentration and the binding rate constant of alendronate to bone.

This model provides a comprehensive understanding of how BPs move through the bone and the time it takes for BP concentration to reach certain levels in the bone. This in turn allows for more accurate dosage times and amounts in order to provide the most efficient bone loss prevention.

Introduction

Background

Osteoporosis, the loss of bone tissue, is a common problem facing astronauts who spend long amounts of time in space. Sustained exposure to zero gravity has been known to increase calcium in the blood, thereby accelerating osteoclast bone resorption. Osteoclast bone resorption is a process which has been closely linked to

osteoporosis and bone loss [1, 2]. In order to assess and ensure a person's health during future long-duration spaceflight missions, a process will need to be developed to combat osteoporosis. Ideally, such a process would be safe and accurate.

There are currently methods for treating osteoporosis through systemic administration of BPs. The drug is highly water soluble and has a short half-life in the blood [3]. Drugs such as BPs have a high binding affinity to hydroxyapatite and as such are able to target large quantities of the molecule found in bone [3]. Once BPs are taken up by osteoclasts, they are metabolized into varying intermediates which all ultimately result in apoptosis of osteoclasts [4].

Oral administration in the form of a pill is one of the simplest and least expensive modes of BP delivery. An advantage of oral drug delivery is its ease of administration. One major disadvantage is the very low absorption of the drug into the bloodstream and ultimate delivery to the bone. According to a recent study by Nakaya et al in 2016, bioavailability of BPs is approximated to be around 1% after consumption, and can be even lower if food is ingested with the drug [5]. In addition, orally administered BPs are known to cause gastrointestinal discomfort [5]. Studies involving alternative delivery methods have attempted to address the various problems associated with oral administration. These alternatives include nasal sprays, intravenous injections, and implants [6]. A more recent method of drug delivery is through the use of a scaffold. A bio-safe bone cement scaffold is often used for

localized administration of drugs. Current procedures involve adding BPs to scaffold bone substitutes in order to target accelerated healing of broken bones [7].

Previous work has attempted to characterize the absorption of BPs in the bloodstream. Such studies aim to limit the concentration of BPs in the blood, which can be dangerous at high concentrations [8]. The absorption and excretion of BPs in blood and urine is well characterized from time of ingestion to time of excretion [6, 8]. It has been shown that BPs have a high affinity for inorganic materials in bone [3], but research into the uptake process is lacking. Previous model work has determined a concentration profile for BPs using constant variables across the bone [10].

Problem Statement

This study is focused on designing a more efficient form of local drug delivery using a scaffold. The scaffold is wrapped around a targeted section of bone. The model uses alendronate, a common type of BP, and a femur bone with dimensions characteristic of an average human male [20].

Initial concentrations of alendronate in the scaffold is increased to study the effect of different initial scaffold concentrations on bound concentrations in the bone. This increase is limited to prevent a dangerous amount of BP from entering the blood stream. The main processes in this study included a mass transfer of drug from the scaffold into the bone, decay of free alendronate as the drug binds to bone, and fluid flow of blood through capillaries in the bone. COMSOL was used to model the physical phenomena and physiological processes that were considered relevant to the drug administration.

Design Objectives

This model geometry was developed to accommodate the following objectives:

- i. Find the time it takes to reach effective concentration (0.1 mM) in compact bone domain [9].
- ii. Determine the time at which over 90% of drug has either left the domain or is in the bound state.
- iii. Determine the bioavailability (fraction of initial drug bound to bone) due to local delivery of alendronate after the time derived in objective 2.

The following assumptions were made in the design of our model in order to accommodate available parameters and implement the model into COMSOL.

- Domain (femur shaft) is approximated as a cylinder
- Domain has three distinct regions with uniform properties in each region
- Drug only diffuses from scaffold into bone
- Scaffold has uniform initial drug concentration of $.018 \text{ mol/m}^3$
- Movement of BP in domain is only due to simple diffusion and convective flow
- Losses of BP from the domain are only through binding and capillaries
- Binding occurs only in the compact bone subdomain
- No saturation of binding sites occurs
- Diffusion from scaffold starts uniformly across scaffold at $t = 0 \text{ s}$
- Blood vessels are modeled as randomly distributed cylinders in the compact bone and periosteum
- Capillaries are the only blood vessels present
- Capillaries in the compact bone extend vertically through the full length of the domain
- Loss of drug from blood vessels in periosteum is approximated as a generalized sink term
- No blood vessels in the marrow

Problem Schematic

Previous work involving BP scaffolds apply the scaffold directly to injured bone to accelerate healing. This study investigates

the effect of wrapping a scaffold around healthy bone to mitigate bone loss. Figure 1 shows a schematic of the design and the process of BP diffusion through the various layers of bone.

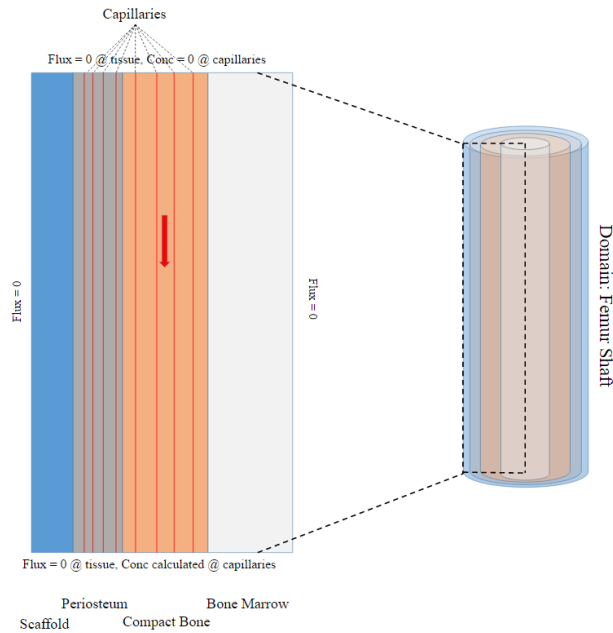


Figure 1: Schematic of model shown as a cross-section of the geometry. Capillaries in periosteum are much closer than capillaries in compact bone.

The bone geometry was modeled as a thin slice of a series of cylindrical shells as shown in Figure 2. The separate cylindrical shells represent discrete layers of bone and are defined as follows: Scaffold is from the outermost shell ($r_o=15.22\text{mm}$, $r_i=15.02\text{mm}$); Periosteum was the next inner shell ($r_o=15.02\text{mm}$, $r_i=14.8\text{mm}$); Compact bone was the next inner shell ($r_o=14.8$, $r_i=13.8\text{mm}$); Bone Marrow was the inner most shell ($r_o=13.8\text{mm}$, $r_i=0\text{mm}$). A thin slice was used in order to reduce the amount of capillaries that had to be implemented to a

number that could be easily integrated into the chosen geometry.

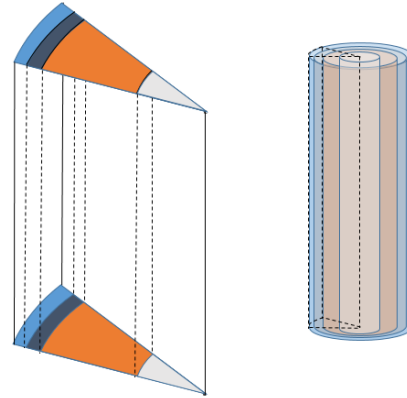


Figure 2: The geometry is modeled as a thin slice of the bone at $\lt; 1^\circ$ (appears as a rectangle in COMSOL because of the small angle).

The model described by Figures 1 and 2 is used to examine BP diffusion into the bone tissue in the femur. This transient 3D model simulates diffusive mass transfer of BP from the scaffold to the bone layers as well as unidirectional convective flow through the capillaries. The domain of the model is the femoral shaft, the section of the femur with the distal and proximal heads removed, and the scaffold that is wrapped around it. All subdomains, with the exception or the capillaries, are modeled as a solid, with the capillaries modeled as pipes with unidirectional flow. As BP diffuses through the tissue, it is bound by the hydroxyapatite in the compact bone. This consumption of BP by the bone in turn decreases the BP concentration in the blood as it flows down the femur.

Methods

Governing Equations

Due to the different processes that are acting in each subdomain, each subdomain has a unique governing equation describing the free alendronate concentration associated with it.

Compact bone:

$$(1) \quad \frac{\partial c}{\partial t} = D \left(\frac{1}{r} \frac{\partial}{\partial r} \left[r \frac{\partial c}{\partial r} \right] + \frac{1}{r^2} \frac{\partial^2 c}{\partial \theta^2} + \frac{\partial^2 c}{\partial z^2} \right) - Kc$$

The compact bone subdomain was modeled as having transient diffusion with a first order reaction term that represents the binding of alendronate in the compact bone (1).

Equation for drug binding:

$$(2) \quad K = -90 \cdot 60 \cdot 60 \cdot 10^{-3} [s^{-1}] \cdot (0 < c)$$

This first order reaction rate was modeled by converting a reaction term from literature [24]. This term was also multiplied by a Boolean operator which ensures that the reaction only happens when the concentration is a real value.

The negation of (2) was used to evaluate the concentration for the bound alendronate in the compact bone.

Capillary:

$$(3) \quad \frac{\partial c}{\partial t} = D \left(\frac{1}{r} \frac{\partial}{\partial r} \left[r \frac{\partial c}{\partial r} \right] + \frac{1}{r^2} \frac{\partial^2 c}{\partial \theta^2} + \frac{\partial^2 c}{\partial z^2} \right) - u_z \frac{\partial c}{\partial z}$$

$$(4) \quad u(r) = u_o \left(1 - \frac{r^2}{R^2} \right)$$

The concentration profile of free alendronate in the capillaries was determined by considering transient diffusion with convection (3). The coupled convection

physics (4) was modeled as pipe flow, as derived from the Navier-Stokes Equation, for efficient computational resource allocation.

Periosteum, Scaffold, Marrow:

$$(5) \quad \frac{\partial c}{\partial t} = D \left(\frac{1}{r} \frac{\partial}{\partial r} \left[r \frac{\partial c}{\partial r} \right] + \frac{1}{r^2} \frac{\partial^2 c}{\partial \theta^2} + \frac{\partial^2 c}{\partial z^2} \right)$$

The concentration profile of free alendronate in the periosteum, scaffold, and marrow subdomains was determined using the equation for cylindrical diffusion (5) due to no alendronate binding or convective flow in these subdomains.

Boundary and Initial Conditions

COMSOL's outflow boundary condition was implemented at the bottom of the capillaries, while a zero-concentration boundary was implemented for the inflow of new blood. The flux value is zero along the rest of the outer edges of the domain.

Table 1: *Initial concentrations of free alendronate in the layers of the modeled domain*

Parameters	Initial Values
C _{capillaries}	0 mg/L
C _{compact}	0 mg/L
C _{periosteum}	0 mg/L
C _{marrow}	0 mg/L
C _{scaffold}	0.018 mol/m ³ [26]

Our model includes zero initial concentrations of free and bound alendronate. The initial concentration of free alendronate in the scaffold was derived from previous literature [26].

Implementation and Mesh Design

A 3D model was created for finite element analysis in COMSOL. The geometry was constructed by extruding a layered wedge of 0.5 degrees of a circle by 100 millimeters. This geometry was modified by the subtraction of several cylinders to create space for the capillaries. These capillaries were later added to the model as separate shapes. The material properties for the domain are listed in the Appendix A. The top of the capillaries were set to a zero concentration. The bottom of the capillaries were given an outflow condition. Following this, a no flux condition was implemented at the remaining boundaries. The initial concentrations are as specified in the previous initial concentrations section.

A swept distribution was used to construct the mesh which is common practice for piped geometries. Our mesh uses standard size parameters from the finer section as follows: Maximum element size 16.5 millimeters, Minimum element size 0.001 millimeters, Maximum element growth rate 1.4, Curvature factor 0.4, Resolution of narrow regions 0.7.



Figure 3: 2D view of mesh

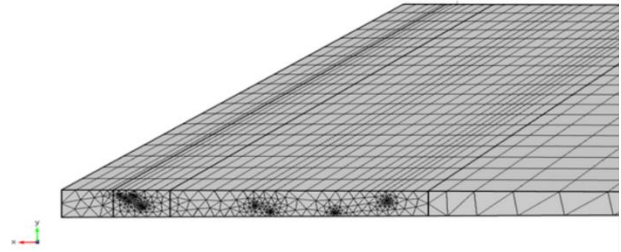
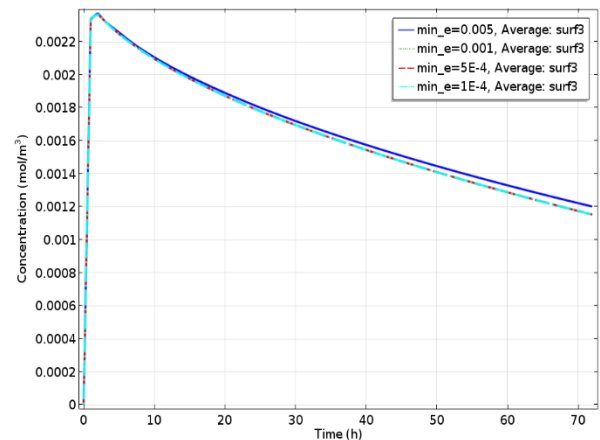


Figure 4: 3D view of mesh

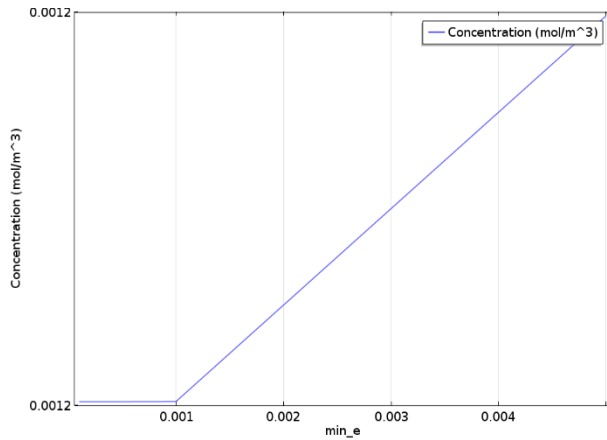
Results and Analysis

Mesh Convergence

The average bound concentration over the compact bone-bone marrow layer was measured to approximate the mesh convergence. Figure 5 displays the mesh convergence by minimum element size. The right plot shows the concentration at a fixed time of 72 hours with varied minimum element size. The plot contains four data points. These plots show that 0.001 millimeter minimum element size is all that is needed for a properly conducted simulation due to there being no change in concentration for smaller minimum element sizes (Fig. 5B).



(A)



(B)

Figure 5: (A) Concentration vs. time for different element sizes. (B) Concentration at compact bone-bone marrow interface vs. minimum element size (72 hours). There is no concentration change for minimum element size smaller than .001 millimeters.

Fluid flow was implemented in COMSOL to model blood flow in the capillaries. Figure 6 shows a plot of the velocity field in the capillaries. The capillary blood flow exhibits laminar parabolic fluid flow. The flow was simplified to parabolic flow to reduce the computation time in COMSOL.

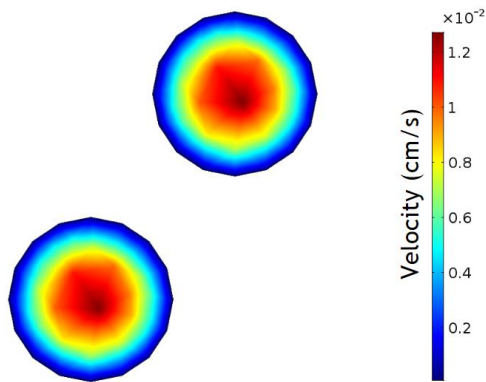


Figure 6: Initial velocity field in capillaries

The concentration of unbound BP was found after 72 hours. Figure 7 displays a cross section of the bone model from the perspective of looking down into the capillaries. The majority of the BP appears to be in the bone marrow at this time. The capillaries carry the drug down toward the bottom of the domain, where it is then removed.

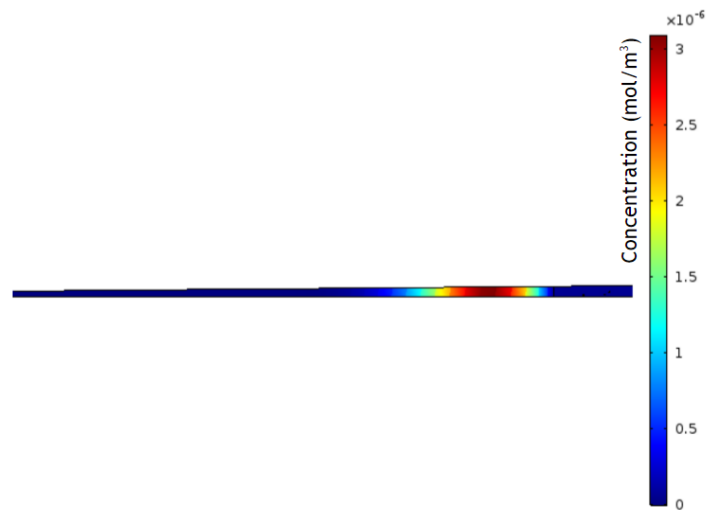


Figure 7: 2D cross section of concentration at 72 hours

In order to see how the concentration of free, or unbound, alendronate changed over time, a plot of average free concentration vs time was obtained.

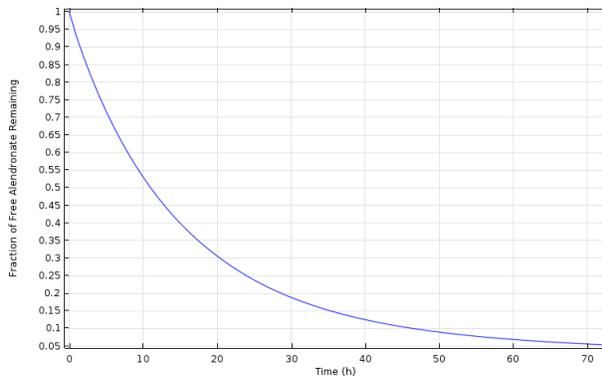


Figure 8: Average concentration of free alendronate in the domain over time

Figure 8 shows the average concentration of free alendronate in the domain over a time period of 72 hours. The concentration decreases rapidly until the end of the time period, in which it approaches zero. The losses of free alendronate in the domain include binding to compact bone and removal by capillaries.

Next, in order to determine the bioavailability of the drug and the severity of its side effects, the rate of BP exiting the domain was investigated. Figure 9 displays the flux of drug out of the domain through the bottom of the capillaries. The amount of unbound drug exiting the bone domain can be used to determine drug concentrations in the blood, which then can be used to determine if safe blood levels are exceeded. The outflow is used to validate the model by comparing the bioavailability to that of experimental data using similar techniques.

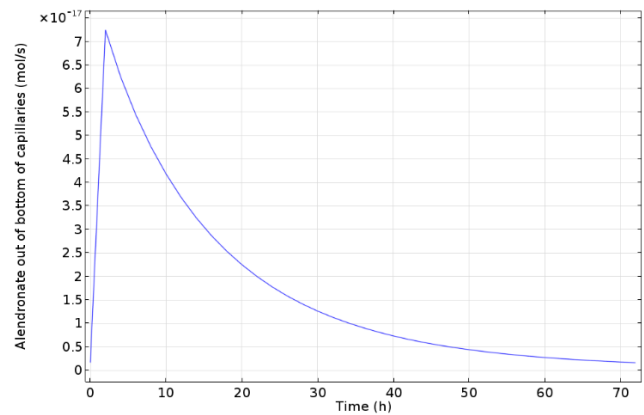


Figure 9: Flux of drug out of bottom of capillaries vs. time

The amount of drug entering blood was investigated in Figure 9. This was calculated via surface integral of the normal concentration multiplied by velocity over the bottom of each unique capillary. The instantaneous concentration is more important in determining the spread of the drug systemically since the half-life of BPs in plasma is about an hour [1].

Model Validation

Our model data as well as experimental data were used to compare bound drug concentrations over time. Figure 10 demonstrated the similar alendronate binding profiles of our model compared to experimental data.

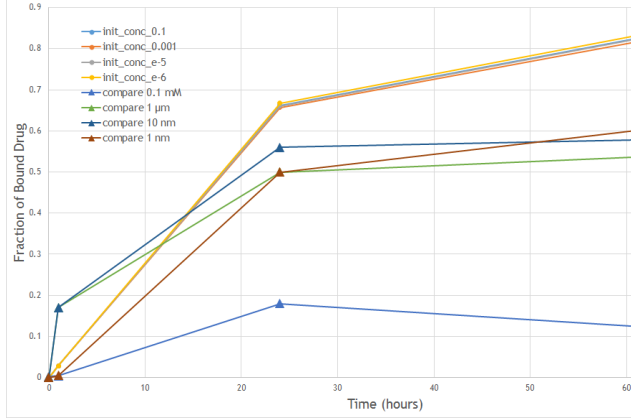


Figure 10: Fraction of drug bound to bone vs. time (From existing paper: [10]) and fraction of drug bound to bone vs. time from COMSOL values

The top four lines represent outputs from our model, while the bottom three lines represent experimental data. The bottom-most line represents a BP dose high enough to cause acute toxicity in patients. This deviation from the expected values of our model as a defect in our model was anticipated. The highest concentration used in the experimental data was intended to show that BPs can saturate binding sites at high concentrations. We have excluded this mechanism from our model since the amount needed to saturate bones is greater than the minimum effective dose by several orders of magnitude. This data is derived from the reaction rate data from COMSOL in the compact bone domain. The data is then averaged over a time interval and multiplied by that time interval. This is performed and summed at the specified points to approximate a time interval.

Figure 10 shows that the bioavailability, or bound fraction of initial drug concentration, of alendronate at clearance time is 90%. This value represents a much higher

bioavailability than the 1% associated with oral administration [5].

Optimization

The probability of bisphosphonate-related toxicity is low, probably because of the drug's rapid plasma and soft tissue clearance [11]. The proposed upper bound of alendronate concentration in the blood to avoid toxic levels is 10^{-4} M [12]. The proposed lower bound, or the effective concentration of alendronate in the bone is 0.1 millimols [9]. Binding was previously demonstrated to last for very long times, with a half-life in bone of over 10 years [25].

Our objective function:

$$(6) J = \Sigma F_b(c_i) + \Sigma F_c(c_j)$$

$$\begin{aligned} F_b(c_i) &= 1, c_i \geq 10^{-4} \\ &= 0, c_i < 10^{-4} \\ F_c(c_j) &= 1000, c_j \geq 10^{-1} \\ &= 0, c_j < 10^{-1} \end{aligned}$$

This objective function is a maximization function whose value increases with bound alendronate above the effective concentration and decreases with free alendronate above the toxic concentration in the blood. The first term $F_b(c_i)$ tracks the volume of compact bone that contains bound alendronate above the effective concentration of 10^{-4} moles and the second term $F_c(c_j)$ tracks the volume of capillary that contains free alendronate above the toxic concentration of 10^{-1} moles at a much higher weighting than $F_b(c_i)$.

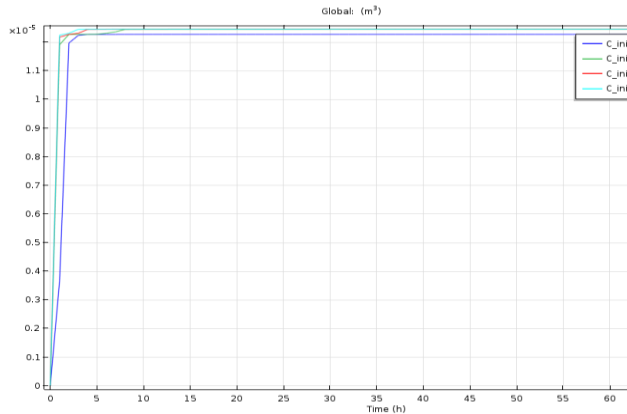


Figure 11: Optimization function over time at several different values of initial concentration

Figure 11 shows that the effective concentration is reached in 99% of the domain by volume over the time period, with this value reaching a steady number in short time. It also shows that the level of toxicity does not change with regard to time or dosage, suggesting that no tissue reaches the toxicity value at these concentrations.

Sensitivity Analysis

A sensitivity analysis was performed to determine the relative importance of certain parameters on the alendronate bound in the compact bone. Parametric sweeps were used to perform these analyses for the values listed in Table 4 of Appendix A.

The sensitivity analysis in Figure 12 shows the percentage change of bound alendronate for both a 20% rise and fall of the tested parameter.

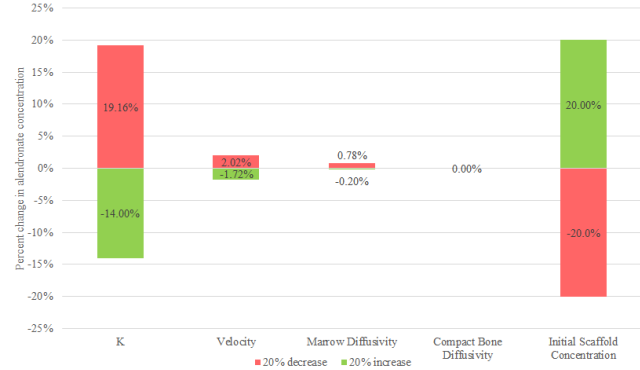


Figure 12: Percentage change in alendronate concentration from varying property and parameter values

The alendronate concentration over 72 hours was most sensitive to changes in the reaction rate as well as the initial scaffold concentration, and least sensitive to the changes in diffusivities in both the compact bone and bone marrow. These results demonstrate that the initial concentration of alendronate is significant when designing the scaffold. Control of the initial drug concentration per unit scaffold area should take precedence in achieving consistent results.

Conclusions

The work in this paper simulates the physiological limitations of a localized delivery of bisphosphonates from a scaffold. Our data on the concentration of drug has shown that the time for this drug to take effect is under 5 hours. Our data also shows that the time for clearance of unbound alendronate from the body is on the order of several days, as previously reported [10]. We also found the fraction of alendronate that binds in the compact bone, a substantial

factor for the bioavailability is very high [10].

More research needs to be performed in order to obtain accurate parameter values for BPs. Many of the parameters used in this paper were for drug analogues or were from animals other than humans. Furthermore, a more accurate rendition of our model may better account for the directionality of blood flow in the femur and may also have a level of interplay and connections between blood vessels. The design of our scaffold, a ring encircling the bone, has yet to be produced and experimentally tested. Most current scaffold are designed as blocks that are

inserted into fractures in bone, though the ring design has no foreseeable restrictions on creation and experimental implementation.

Appendix A

Parameters

Table 2: Model Parameter Values

Parameter	Value	Source
Radial thickness of bone marrow (r_m)	0.0138 m	[31]
Radial thickness of compact bone (r_c)	0.001 m	[30]
Radial thickness of periosteum (r_p)	2.2e-4 m	[29]
Radial thickness of scaffold (r_s)	200 μ m	[33]
Radius of capillary (r_{ca})	4 μ m	[21]
Diffusivity of compact bone (D_c)	150e-12 m ² /s	[23]
Diffusivity of bone marrow (D_m)	1e-12 m ² /s	[18]
Diffusivity of periosteum (D_p)	2.44e-10 m ² /s	[22]

Diffusivity of scaffold (D_s)	115e-12 m ² /s	[15]
Diffusivity of blood (D_b)	7.8e-11 m ² /s	[32]
Density of compact bone (ρ_c)	1.901 g/cm ³	[27]
Density of bone marrow (ρ_m)	1.200 g/cm ³	[27]
Density of blood (ρ_b)	1060 kg/m ³	[28]
Binding rate constant (K)	90*10 ⁻³ 1/hr	[24]
Distance between capillaries	100-150 um center to center	[21]

Table 3: COMSOL Variables

Variable Name	Description
velocity	Velocity of blood in capillary
min_e	Minimum element size for mesh
D_bone	Diffusivity of compact bone
C_init	Initial concentration in scaffold

Table 4: Sensitivity Analysis Parameters

Parameter	-20% of original value	+20% of original value
Compact Bone Diffusivity	1.2e-10 m ² /s	1.8e-10 m ² /s
Initial Scaffold Concentration	0.0144 mol/m ³	0.0216 mol/m ³
Blood Velocity	40 um/s	60 um/s
Bone Marrow Diffusivity	1.2e-12 m ² /s	1.8e-10 m ² /s

Appendix B

CPU Time

```
Time-stepping completed.
Time-Dependent Solver 1 in Study 1/Solution 1 (sol1): Solution time: 1311 s (21 minutes, 51 seconds)
Physical memory: 2.08 GB
Virtual memory: 2.26 GB
=====
```

References

- [1] Fleisch, H. (2000). BPs in bone disease: from the laboratory to the patient. Academic press.
- [2] Cavanagh, P. R., Licata, A. A., & Rice, A. J. (2007). Exercise and pharmacological countermeasures for bone loss during long duration space flight. *Gravitational and Space Research*, 18(2).
- [3] Hirabayashi, H., & Fujisaki, J. (2003). Bone-specific drug delivery systems. *Clinical pharmacokinetics*, 42(15), 1319-1330.
- [4] Li, B., Chau, L., Fung, J., Wang, X., & Leong, W. F. (2011). Bisphosphonates, specific inhibitors of osteoclast function and a class of drugs for osteoporosis therapy. *Journal of cellular biochemistry*, 112(5), 1229-1242.
- [5] Nakaya, Y., Takaya, M., Hinatsu, Y., Alama, T., Kusamori, K., Katsumi, H., ... & Yamamoto, A. (2016). Enhanced Oral Delivery of BP by Novel Absorption Enhancers: Improvement of Intestinal Absorption of Alendronate by N-Acyl Amino Acids and N-Acyl Taurates and Their Absorption-Enhancing Mechanisms. *Journal of pharmaceutical sciences*, 105(12), 3680-3690.
- [6] Ezra, A., & Golomb, G. (2000). Administration routes and delivery systems of BPs for the treatment of bone resorption. *Advanced drug delivery reviews*, 42(3), 175-195.
- [7] Cattalini, J. P., Boccaccini, A. R., Lucangioli, S., & Mouriño, V. (2012). Bisphosphonate-based strategies for bone tissue engineering and orthopedic implants. *Tissue Engineering Part B: Reviews*, 18(5), 323-340.
- [8] Phadungsombut, N., Chuchome, T., & Wiwattanawongsa, K. (2013). Pharmacokinetics of alendronate in a combined Alendronate/Vitamin D 3 tablet in healthy volunteers using plasma and urine data. *Songklanakarinn Journal of Science & Technology*, 35(3).
- [9] Sato, M., Grasser, W., Endo, N., Akins, R., Simmons, H., Thompson, D. D., ... & Rodan, G. A. (1991). Bisphosphonate action. Alendronate localization in rat bone and effects on osteoclast ultrastructure. *Journal of Clinical Investigation*, 88(6), 2095.
- [10] Blair, H. C., Teitelbaum, S. L., Tan, H. L., & Schlesinger, P. H. (1992). Reversible inhibition of osteoclastic activity by bone-bound gallium (III). *Journal of cellular biochemistry*, 48(4), 401-410.
- [11] Fleisch, H. (1993). New bisphosphonates in osteoporosis. *Osteoporosis international*, 3, 15-22.
- [12] Gangoiti, M. V., Cortizo, A. M., Arnol, V., Felice, J. I., & McCarthy, A. D. (2008). Opposing effects of bisphosphonates and advanced glycation end-products on osteoblastic cells. *European journal of pharmacology*, 600(1), 140-147.

- [13] Treece, G. M., Gee, A. H., Mayhew, P. M., & Poole, K. E. S. (2010). High resolution cortical bone thickness measurement from clinical CT data. *Medical image analysis*, 14(3), 276-290.
- [14] Huang, B. W., Chang, C. H., Wang, F. S., Lin, A. D., Tsai, Y. C., Huang, M. Y., & Tseng, J. G. (2012). Dynamic characteristics of a hollow femur. *Life Science Journal*, 9(1), 723-726.
- [15] Fronck, A., Criqui, M. H., Denenberg, J., & Langer, R. D. (2001). Common femoral vein dimensions and hemodynamics including Valsalva response as a function of sex, age, and ethnicity in a population study. *Journal of vascular surgery*, 33(5), 1050-1056.
- [16] Leblanc, A., Matsumoto, T., Jones, J., Shapiro, J., Lang, T., Shackelford, L., ... & Sibonga, J. (2013). BPs as a supplement to exercise to protect bone during long-duration spaceflight. *Osteoporosis International*, 24(7), 2105-2114.
- [17] Henneman, Z. J., Nancollas, G. H., Ebetino, F. H., Russell, R. G. G., & Phipps, R. J. (2008). BP binding affinity as assessed by inhibition of carbonated apatite dissolution in vitro. *Journal of Biomedical Materials Research Part A*, 85(4), 993-1000.
- [18] DiResta GR and Healey JH. Mathematical Model and Experimental Validation of Local Delivery of Pamidronate to Bone Adjacent to Pamidronate –PMMA Bone Cement. Memorial Sloan Kettering Cancer Center. 51st Annual Meeting of the Orthopaedic Research Society.
- [19] Barrio, M., & Raghunandan, S. (2011, October 28). *Modeling the Diffusion of TGF- β 1 from a Fibrin Scaffold through Alveolar Bone* [Scholarly project]. Retrieved from BENG 221 Mathematical Methods in Bioengineering
- [20] Dayal, Manisha R., Steyn, Maryna, & Kuykendall, Kevin L.. (2008). Stature estimation from bones of South African whites. *South African Journal of Science*, 104(3-4), 124-128. Retrieved May 11, 2017, from http://www.scielo.org.za/scielo.php?script=sci_arttext&pid=S0038-23532008000200010&lng=en&tlng=en.
- [21] Zahm, A. M., Bucaro, M. A., Ayyaswamy, P. S., Srinivas, V., Shapiro, I. M., Adams, C. S., & Mukundakrishnan, K. (2010). Numerical modeling of oxygen distributions in cortical and cancellous bone: oxygen availability governs osteonal and trabecular dimensions. *American Journal of Physiology-Cell Physiology*, 299(5), C922-C929.
- [22] Heli, H., Faramarzi, F., & Sattarahmady, N. (2010). Voltammetric investigation and amperometric detection of the bisphosphonate drug sodium alendronate using a copper nanoparticles-modified electrode. *Journal of Solid State Electrochemistry*, 14(12), 2275-2283.
- [23] Martínez, I. (n.d.). *Mass Diffusion*. Lecture presented at Isidoro Martínez' lectures on Heat and Mass Transfer. Retrieved from <http://webserver.dmt.upm.es/~isidoro/bk3/c11/index.htm>
- [24] Nieto, A. Balas, F. Et al. (2008) Functionalization degree of SBA-15 as key factor to modulate sodium alendronate dosage. *Microporous and Mesoporous Materials*. 116(1-3), 4-13.

- [25] Rodan, G. A., & Fleisch, H. A. (1996). Bisphosphonates: mechanisms of action. *Journal of Clinical Investigation*, 97(12), 2692.
- [26] Boanini, E., Torricelli, P., Gazzano, M., Giardino, R., & Bigi, A. (2008). Alendronate–hydroxyapatite nanocomposites and their interaction with osteoclasts and osteoblast-like cells. *Biomaterials*, 29(7), 790-796.
- [27] Blanton, P. L., & Biggs, N. L. (1968). Density of fresh and embalmed human compact and cancellous bone. *American journal of physical anthropology*, 29(1), 39-44.
- [28] Cutnell, J. & Johnson, K. (1998). *Physics, Fourth Edition*.
- [29] Manzar H, Antonios TT, Adds PJ (2016) Periosteal Thickness around the Femoral Neck: a cadaveric study. *J Clin Exp Orthop* 2: 17. doi: 10.4172/2471-8416.100017
- [30] Treece, G. M., Gee, A. H., Mayhew, P. M., & Poole, K. E. S. (2010). High resolution cortical bone thickness measurement from clinical CT data. *Medical Image Analysis*, 14(3), 276–290. <http://doi.org/10.1016/j.media.2010.01.003>
- [31] B. W. Huang, C.H. Chang, F.-S. Wang, A.D. Lin, Y.C. Tsai, M.Y. Huang, J.-G. Tseng. Dynamic Characteristics of a Hollow Femur. *Life Science Journal* 2012; 9(1):723-726]. (ISSN: 1097-8135). <http://www.lifesciencesite.com>. 104.
- [32] Zahm, A. M., Bucaro, M. A., Ayyaswamy, P. S., Srinivas, V., Shapiro, I. M., Adams, C. S., & Mukundakrishnan, K. (2010). Numerical modeling of oxygen distributions in cortical and cancellous bone: oxygen availability governs osteonal and trabecular dimensions. *American Journal of Physiology - Cell Physiology*, 299(5), C922–C929. <http://doi.org/10.1152/ajpcell.00465.2009>
- [33] Mishra, S. (2017). A fresh look at bioresorbable scaffold technology: Intuition pumps. *Indian Heart Journal*, 69(1), 107-111. doi:10.1016/j.ihj.2017.01.006